Correlations and fluctuations in phase coarsening

K. G. Wang,[1] M. E. Glicksman,[1] and Chaogang Lou[2]
[1]*Materials Science and Engineering Department, Rensselaer Polytechnic Institute, Troy, New York 12180, USA*
[2]*Department of Electronic Engineering, Southeast University, Nanjing 210096, People's Republic of China*
(Received 22 November 2005; revised manuscript received 8 March 2006; published 2 June 2006)

Three-dimensional phase coarsening at various volume fractions is simulated by employing multiparticle diffusion methods. The dynamic process of phase coarsening is visualized through a three-dimensional movie. The present study also characterizes interparticle spacings in polydispersed particle systems and clarifies the controversial mathematical expressions for interparticle spacings used in the literature for 30 years. Consequently, this study reveals spatial, temporal, and nearest-neighbor correlations in polydispersed particle systems. A new three-dimensional movie of a Voronoi network demonstrating these correlations is provided. Our simulation and experiments show that growth rates of individual particles deviate from those of the mean-field theory, which is caused by their differing local environments. Multiplicative noise provides a good basis to describe the stochastic nature of fluctuations during phase coarsening.

DOI: 10.1103/PhysRevE.73.061502 PACS number(s): 64.75.+g, 81.30.Mh, 05.40.Ca, 64.60.−i

Phase coarsening, or Ostwald ripening, is a ubiquitous phenomena occurring in the fields of chemistry, physics, materials science, geology, and economics. In a typical phase separation process, nucleation, growth, and, eventually, phase coarsening, all usually follow a temperature quench from an initially homogeneous phase that eventually results in a well-separated two-phase microstructure. Specifically, nucleation of a second phase occurs within a supersaturated solution, followed by its growth. In the late stage of phase separation, the onset of competitive coarsening occurs among the precipitate particles, so phase coarsening sets in. Phase coarsening—i.e., the growth of the average size particle—occurs at the expense of small particles within a system, which shrink even further and finally disappear. Extensive interest has arisen in recent years to develop the architecture and fabrication techniques for producing nanostructured and microstructured materials.

The control of size, shape, location, and particle size distribution (PSD) of nanocrystallites via phase coarsening is important, for example, to achieve the synthesis of colloidal semiconductor nanocrystals [1–4]. Applications of these types of functional materials appear to be remarkably diverse, ranging from controlled drug delivery and protection of biologically active agents, photonic crystals, nanocatalysts, elastomeric fillers, etc. [3]. These applications can be achieved through manipulation of the kinetics of phase separation, which requires a deep understanding of phase coarsening processes. The computational modeling of phase coarsening occurring in three spatial dimensions requires sufficiently large enough systems to yield statistically meaningful data. At present, achieving accurate simulations of such large microstructures remains a daunting computational task. For example, only scant attention was paid to the underlying kinetics mechanism—i.e., Ostwald ripening—which is responsible for the evolution and self-assembly of quantum dots, or island crystallites, formed on surfaces in some semiconductor nanomaterials. The average center-to-center interparticle spacing in dispersed systems is an important parameter of materials encountered in a wide variety of conventional metallurgical and nanomaterials. Nevertheless, there remain controversial mathematical expressions that have been posed in the literature on this subject for over 30 years [5–8]. Indeed, the magnetic, electronic, catalytic, and mechanical properties of materials depend on the microstructure's average particle size, PSD, and its spatial and temporal correlations.

Three-dimensional phase coarsening at various volume fractions is simulated, and a three-dimensional movie derived from the simulation data demonstrates the dynamic process of phase coarsening. Through simulation, we clarify the correct choice among conflicting mathematical expressions for predicting interparticle spacings in polydispersed particle systems. Spatial, temporal, and nearest-neighbor correlations during phase coarsening are carefully characterized and then demonstrated in a movie of a three-dimensional Voronoi network created for this paper. Relationships between the growth rates of individual particles and their differing local environments are established. The concepts and results given here can provide useful guidance where competitive phase growth occurs in such applied physics contexts such as nanoscience and microstructure evolution.

The first quantitative description of the statistical mechanics of phase coarsening was a mean-field theory developed by Lifshitz and Slyozov [9], and then by Wagner [10]. This theory, often referred to as LSW theory, retains full validity only in the limit of a vanishingly small volume fraction of dispersoid, because of the exclusion of *all* physical interactions among the particles. As shown in numerous experiments, the well-known scaling prediction from the LSW theory that the cube of the average length scale of the dispersed particles increases linearly with time remains valid, even in cases of finite volume fraction V_V, where particles clearly interact. Specifically, the LSW theory predicts that particles with identical sizes have the identical volume fluxes, regardless of their individual location within the microstructure. The volume flux derived from the LSW theory is usually written as the linear form

$$B_{LSW}(\rho) = 1 - \rho, \tag{1}$$

where the normalized radius of a particle, $\rho \equiv R/\langle R \rangle$, is the particle radius R, normalized by the average radius of the particle population $\langle R \rangle$.

In the case of nonzero volume fraction, the diffusional interaction among particles needs to be accounted for, and it has been studied by several investigators. Ardell [11], for example, modified the LSW theory and considered the influence of nearest neighbors on the growth rate of particles. His detailed results, however, seem to overestimate the influence of the volume fraction. Variations on Ardell's method, however, have been implemented by Tsumuraya and Miyata [12] using a series of different kinetic coarsening interaction laws, referred to as TM models. Specifically, each TM model defines some appropriate "radius of influence" around each particle. All of the TM models, however, employed heuristic extensions of the basic mean-field LSW approach. Brailsford and Wynblatt [13] were the first to employ the "effective medium" theory to study phase coarsening. They obtained growth rates of the particles and a broadened PSD, and established an implicit relationship between the coarsening rate and volume fraction. Marsh and Glicksman [14] then introduced the concept of a statistical "field cell" acting around each size class of the particles undergoing phase coarsening, and obtained coarsening rates. All of the theoretical models mentioned above employed growth rate equations based on using Laplace's equation as the quasistatic approximation for the time-dependent diffusion field. Marqusee and Ross [15], by contrast, limited the spatial extent of the diffusion field by taking into account "screening" provided by a two-phase medium comprised of the matrix and a distribution of particles considered to be a globally neutral system of diffusion point sources and sinks. Instead of using Laplace's equation as the quasistatic approximation, Marqusee and Ross showed that Poisson's equation is appropriate for deriving a suitable kinetic expression for the growth rates in an "effective medium." Marder [16] examined the effect of diffusive interactions and correlations between particles. Kawasaki and coworkers studied the Ostwald ripening on the basis of a new dynamical interfacial model [17–20].

One may describe the many-body interactions among particles for microstructures with nonzero volume fractions of the dispersed phase by introducing an additional length scale, the diffusion screening length ρ_0. This screening distance, which is a collective property of the microstructure, limits the extent of particle-particle diffusive interactions. It may be shown [21] that the diffusive screening distance in coarsening is

$$\rho_0 = \sqrt{\frac{\langle \rho^3 \rangle}{3\langle \rho \rangle V_V}}. \tag{2}$$

The diffusional screening length defined in Eq. (2) sets the maximum range over which the interactions occur, and beyond which such interactions cease. This length scale is analogous to the Debye screening distance for electrostatic interactions in dilute ionized plasmas. In addition, it was proved that the many-body diffusive interactions among particles increase the volume flux, $B(\rho)$, beyond that predicted by the LSW theory [21]. Specifically, it was shown that the diffusion screening distance affects the volume flux of particles as

$$B(\rho) = B_{LSW}(\rho)\left(1 + \frac{\rho}{\rho_0}\right). \tag{3}$$

The earliest attempt to simulate multiparticle diffusion using numerical methods occurred in 1973 by Weins and Cahn [22], whose simulation system includes just a few interacting particles arranged in several configurations to demonstrate basic coarsening interactions. Following this work, Voorhees and Glicksman [23] systematically studied the behavior of several hundred particles randomly distributed in a three-dimensional unit cell to simulate microstructural phase coarsening. Later, Beenaker [24] enhanced the capability of multiparticle diffusion simulation procedures and was able to increase the total number of particles during simulation to several thousand. Other investigators [21,25,26], continued to improve upon the accuracy and statistical basis of large-scale simulations of late-stage phase coarsening. The three-dimensional microstructure evolution for various volume fractions was simulated using multiparticle diffusion methods by placing n particles of the dispersoid phase within a cubic computational box [21]. The contiguous spaces between particles represent the matrix phase, in which the dispersoid population is embedded, and through which solute diffuses. Particles are located by specifying the positions of their centers and by their radii. Some additional simplifying assumptions were employed in the simulations: (1) the kinetics of coarsening was determined solely by volume diffusion through the contiguous matrix and (2) solute transport to or from each phase domain occurred sufficiently slowly to be approximated as quasistatic. These assumptions allow solute diffusion in the matrix to be represented by Laplace's equation. Thus, the concentration field $\mathcal{C}(\mathbf{r})$ in the matrix obeys $\nabla^2\mathcal{C}(\mathbf{r})=0$, where the dimensionless concentration is defined here as $\mathcal{C}(\mathbf{r}) \equiv [c(\mathbf{r})-c_0]/c_0$. The quantity $c(\mathbf{r})$ is the actual concentration of the matrix phase at the position, $\mathbf{r}$, and c_0 denotes the equilibrium solubility established at a flat interface between the matrix and particle phases at the coarsening temperature and pressure. The boundary condition applied at the spherical interface of the ith particle is specified through the Gibbs-Thomson local equilibrium solubility relation, namely, $\mathcal{C}(R_i)=1/R_i$, where R_i is the nondimensional radius of the ith particle scaled by the system's capillary length [21].

The solution to Laplace's equation for n particles may be represented as the superposition of n dimensionless concentration fields [21]. The global mass conservation law for a microstructure represented by such a discrete two-phase system may be expressed through the closure condition on the total solute flux, $\Sigma_{i=1}^{n} 4\pi B_i = 0$, where the ith particle's volume flux is $4\pi B_i$. The relationship establishing the far-field concentration in the matrix phase expresses a microstructural response that includes local interactions among particles. More specifically, the far-field potential depends explicitly on the particle positions and the distances between every particle pair. Moreover, the far-field concentration requires an inclusion of detailed environmental information, including a description of the locale of every particle. More importantly, the far-field concentration, which depends on the local arrangement of particles, confers subtle influences on a given particle's rate of diffusion-limited growth or shrinkage [21].

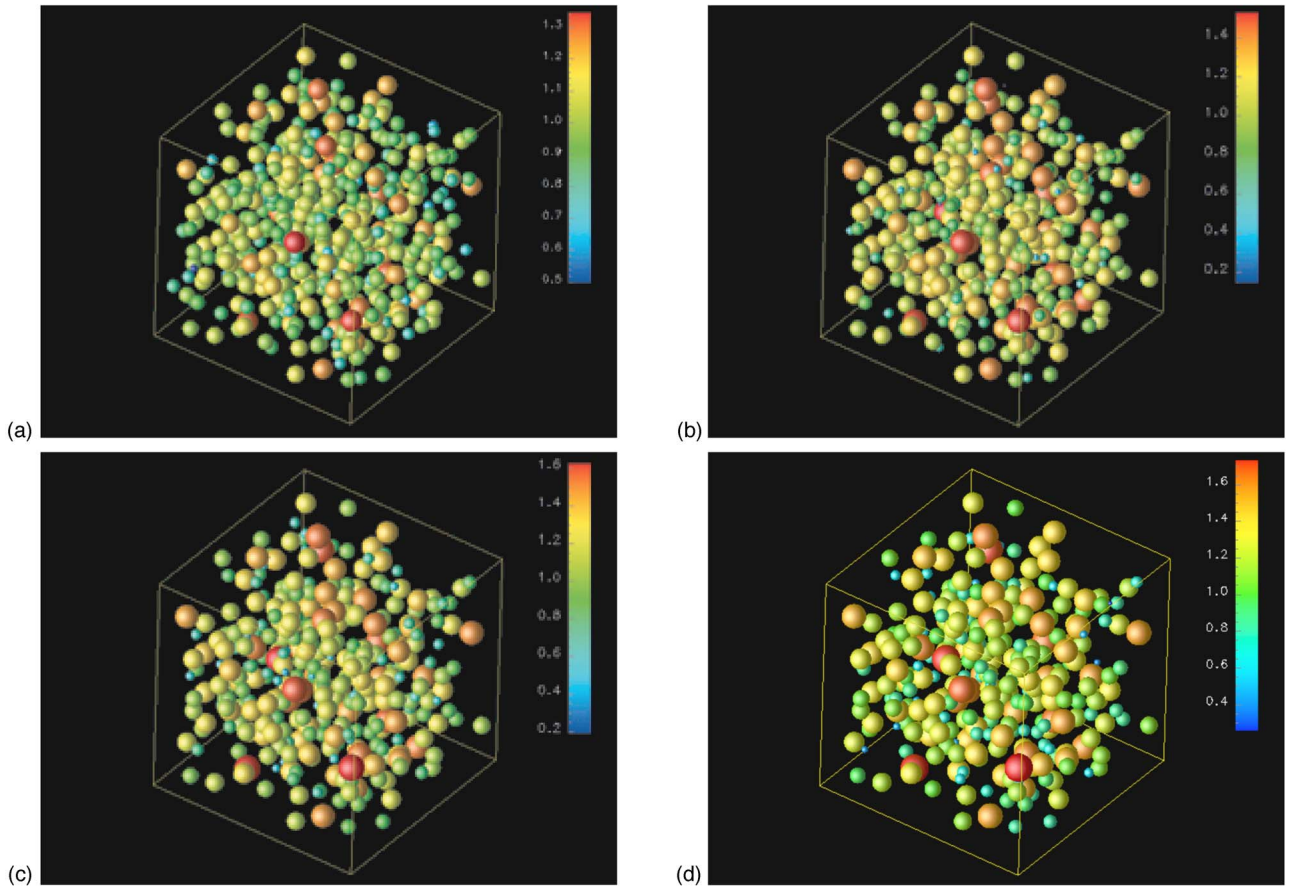

FIG. 1. (Color online) Simulated microstructures: (a) upper left, initial state (computer times) $t=0$; (b) upper right, $t=0.25$; (c) lower left, $t=0.5$; and (d) lower right, end of simulation, $t=1.0$. The sizes of these particles are indexed by color.

The dimensionless form of the growth rate of the ith particle, can be expressed as

$$\frac{dR_i}{dt} = -\frac{B_i}{R_i^2} \quad (i = 1,2,\ldots,n), \tag{4}$$

where R_i is known at the evolution time t. Here time is nondimensionalized by a characteristic diffusion time [21]. The Runge-Kutta method was used to integrate numerically the n growth rate expressions, Eq. (4). The coarsening process is represented by a system of linear equations using the solution to Laplace's equation and the Gibbs-Thomson boundary conditions for n particles. This large linear system of equations may be cast into the matrix form as

$$\mathbf{A}' \cdot \mathbf{B}' = \mathbf{U}', \tag{5}$$

where $\mathbf{A}'$, $\mathbf{B}'$, and $\mathbf{U}'$ are, respectively, $n \times n$ $n \times 1$ and $n \times 1$ matrices. Expressions for these matrices may be found elsewhere [21]. The Gauss-Seidel method was employed to solve this linear system, Eq. (5), yielding at each time step updated values for the volume fluxes B_i. Substitution of the updated B_i values back into Eq. (4) dynamically advances the coarsening system by updating the radii of all the active particles and their coordinates.

Microstructures were simulated, consisting of dispersoid volume fractions of $V_V = 10^{-10}$, 10^{-4}, 10^{-3}, 10^{-2}, 0.1, 0.2, and 0.3. In this range of volume fractions, there are no direct mergers of particles in these simulations. The evolution of a typical three-dimensional microstructure simulated by the methods described above is shown in Fig. 1, for $V_V = 0.1$. Specifically, Figs. 1(a)–1(d) show simulations of three-dimensional microstructures evolving over time. A comparison of these microstructures clearly elucidates the progress of phase coarsening, as small particles shrink, large particles grow, and their overall number density decreases. Small particles located in the upper-right corner of the initial frame [Fig. 1(a)] shrink and disappear by the final frame [Fig. 1(d)]. A movie for the microstructural evolution is available on supporting online (see movie S1). The movie and images provide an opportunity for theorists and experimentalists to compare microstructural evolution quantitatively as observed in experiments and simulations.

Resolving the issue of interaction length scales allows us considerable clarification of the fundamental nature of diffusion-limited phase coarsening kinetics occurring in microstructures. One could, for example, study the spatial and nearest-neighbor correlations using the simulation data obtained at different volume fractions. For example, the pair correlation functions were obtained for these microstructures, which provide a measure of the average separation distance between a given particle and its nearest neighbor. In the initial configuration, different sized particles were randomly placed within a cubic box and allowed to evolve by

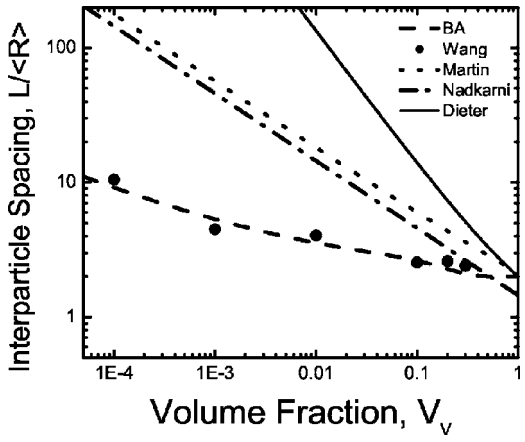

FIG. 2. Average interparticle spacing distance from different authors. Filled circles represents our results from simulations. Solid, dashed, dotted, and dotted-dashed lines represent the approximation results from Dieter [8], Bansal and Ardell [5], Martin [6], and Nadkarni [7], respectively.

multiparticle diffusion. The pair correlation functions were determined in the initial configuration and at the termination of the simulation for each volume fraction. Peak positions of the pair correlation functions were found for each case. The peak position of the pair correlation equals the average center-to-center distance between a particle and its nearest neighbor. The average center-to-center distances for $V_V = 10^{-4}$, 10^{-3}, 10^{-2}, 0.1, 0.2, and 0.3, are plotted in Fig. 2. The average center-to-center distance between a particle and its nearest neighbor in dispersed systems provides a useful parameter encountered in a variety of metallurgical and colloidal materials. Formerly, calculating the center-to-center distance between a particle and its nearest neighbor in dispersed systems has proven to be difficult. For example, Bansal and Ardell [5] derived the following formula for the interparticle spacing in a three-dimensional distribution of finite spheres:

$$\frac{L_{BA}}{\langle R\rangle} = 2 + \frac{e^{8V_V}}{3V_V^{1/3}}\Gamma\left(\tfrac{1}{3}, 8V_V\right), \tag{6}$$

where Γ denotes the Gamma function. Martin [6] also independently estimated the interparticle spacing as

$$\frac{L_M}{\langle R\rangle} = 1.23\sqrt{\frac{2\pi}{3V_V}} - 2\sqrt{\tfrac{2}{3}} + 2, \tag{7}$$

whereas Nadkarni [7] claimed that the interparticle spacing may be represented as

$$\frac{L_N}{\langle R\rangle} = \sqrt{\frac{2\pi}{3V_V}}. \tag{8}$$

Finally, in his textbook, Dieter [8] gave the following expression for the interparticle spacing:

$$\frac{L_D}{\langle R\rangle} = \frac{4}{3}\left(\frac{1}{V_V} - 1\right) + 2. \tag{9}$$

A comparison of all these theoretical estimates, Eqs. (6)–(9), with the simulation data presented in Fig. 2 shows that Bansal and Ardell's prediction, Eq. (6), provides the best agreement with the multiparticle diffusion simulations. Figure 2 also shows that the three other theoretical estimates based on expressions by Martin, Nadkarni, and Dieter differ substantially from the simulations and from Bansal and Ardell's analytic approximation. The disparity worsens at small volume fractions. The formulas of Martin, Nadkarni, and Dieter, nevertheless, are broadly adopted in many current applications of phase coarsening. Now, after more than 30 years, accurate simulations and theory may be compared critically as to which the theory provides the most reliable predictions of microstructures. The simulation data presented in this paper indicate that the interparticle spacings in dispersed systems predicted by Bansal and Ardell are accurate, and, in our opinion, should be used in place of the approximations suggested by Martin, Nadkarni, and Dieter.

The nearest-neighbor spacings in a network structure may be determined by the well-known Voronoi construction. Figure 3 shows the Voronoi construction on a cross section taken through the cubic simulation box. The filled circles in Fig. 3 represent the areas of individual particles, which are present in this instance at a volume fraction of $V_V = 0.1$. Ostwald ripening of a microstructure may be described qualitatively as the atom exchange occurring between nearest neighbors through the walls of the intervening Voronoi cell. Therefore, the diffusion-limited solute flux flowing between particles is related to the geometry of the local Voronoi cell. Thus, one finds that the growth rate of an individual particle is related to its relative position among neighbors, their individual radii, and the shape of the participating Voronoi cell. Local correlations, suggested by the Voronoi cell, relate the growth rates and interactions among nearby particles. The evolution of the three-dimensional Voronoi network with time is available on supporting online (see movie S2). From it, one can learn how the average volume of Voronoi cells changes with time, and the dynamic processes of the local environment of every particle.

One can observe and measure accurately, using the current simulation method, the individual growth rates or volume flux of every particle in the microstructure. Of special interest here is that the simulations also reveal that the volume flux of the particles are all different—even for particles with the same radii, given that they are located in differing microstructural environments, or locales. Figure 4 shows the volume fluxes $B(\rho)$ simulated for a two-phase microstructure with $V_V = 0.2$. For comparison, the volume fluxes predicted from the LSW theory, Eq. (1), and from diffusion screening theory, Eq. (3), appear together in Fig. 4. Figure 4 clearly demonstrates that the average volume flux predicted from the diffusion screening theory deviates steadily from the linear, mean-field, LSW prediction, which lacks any consideration of the influence of the volume fraction of the microstructure and the concomitant interactions. Simulations conducted with different volume fractions show that the nonlinear char-

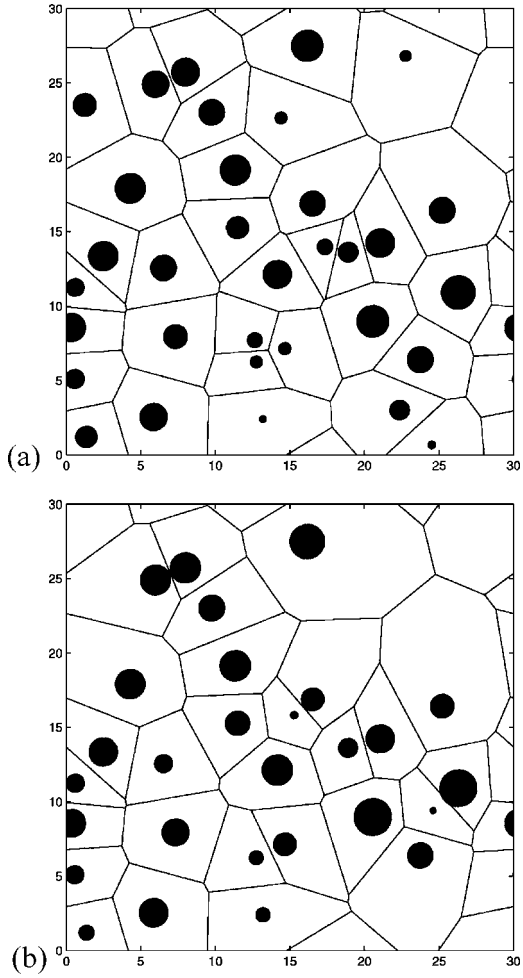

FIG. 3. Voronoi construction using multiparticle diffusion simulation data for coarsening at $V_V=0.1$. Black circles represent the dispersed particles in the matrix. (a) Voronoi network at the beginning of simulation, (b) Voronoi network at the termination of simulation.

acter of the particle volume flux versus particle radius increases steadily with increasing volume fraction. Moreover, even particles with identical size exhibit a wide variation of the volume flux, B_i. This result shows that the growth rates of identical sized particles can differ from that of the mean-field prediction, because growth rates are proportional to the volume fluxes via Eq. (4). As suggested, the deviations from the mean flux arise from the differing microstructural environments surrounding each particle. Experimental results, [28,29], also confirm these effects. The term "locale fluctuations" is used to describe such deviations. However, locale fluctuations in the current context of stochastic coarsening kinetics are not at all related to thermal noise or thermodynamic fluctuations, but rather to local arrangements of particles and the correlations attending those arrangements.

In addition, we consistently observed that larger particles $R \geq \langle R \rangle$ experience in their growth rates stronger locale fluctuations than do small particles, $R \ll \langle R \rangle$. The variation of the dispersion of growth rates with a particle size is caused by the relative localization of the diffusion field surrounding small particles. This observation further suggests that locale

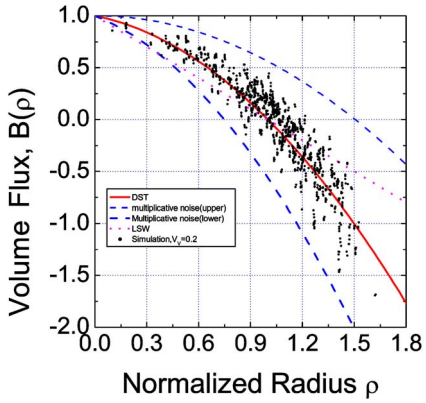

FIG. 4. (Color online) Volume flux $B(\rho)$ versus scaled particle radius ρ. Data are from simulations at $V_V=0.2$. Red (solid), magenta (dotted), and blue (dashed) lines represent volume fluxes from diffusion screening theory [21], LSW theory, and upper and lower bands [see Eq. (11)], respectively.

fluctuations are correlated strongly with the size of a particle and the volume fraction of the microstructure. We recently developed estimates of the expected fluctuation bands using the statistical sampling theory [27]. The following stochastic expression was found for the fluctuation of the particle volume flux:

$$\zeta\left(\frac{\rho}{\rho_0}\right) = \frac{\rho}{2\rho_0}\left(1 + \frac{\rho}{\rho_0}\right)\eta. \tag{10}$$

Here η is a Gaussian random variable with mean-value zero and unit width, and $\zeta(\rho/\rho_0)$ is the Gaussian multiplicative fluctuation. In Fig. 4, all the simulation data scatter within the predicted bands, showing that the Gaussian multiplicative noise provides a reasonable match with the simulations. Considering that there exists a spectrum of fluctuations in the volume fluxes, one must consider adding a multiplicative fluctuation term to the theoretical expression for the volume fluxes, Eq. (3). The resulting stochastic expression for a particle's volume flux becomes

$$B(\rho) = B_{LSW}\left(1 + \frac{\rho}{\rho_0}\right) + \frac{\rho}{2\rho_0}\left(1 + \frac{\rho}{\rho_0}\right)\eta. \tag{11}$$

A stochastic differential equation may be derived from Eq. (11) that describes the growth rates of coarsening particles [27]. This equation provides the kinetic evolution law for particles in a "noisy" microstructure.

Three-dimensional phase coarsening was simulated for a range of volume fractions, and the process of three-dimensional phase coarsening was visualized within a movie. However, most experiments cannot provide three-dimensional visualization of phase coarsening, but rather provide TEM images, which are two-dimensional projections that lose some spatial information. To our knowledge the two-phase binary alloys based on Al-Li provides a nearly ideal binary alloy system for kinetic study, because the δ' particles in this alloy have a small lattice misfit with the solid solution matrix phase, thus contributing a negligible amount of strain-induced free energy to the coarsening process. Gu

et al. [30] first studied phase coarsening kinetics in Al-Li alloys, employing quantitative transmission electron microscopy (TEM). Then Mahalingam *et al.* [31] studied coarsening of $\delta' - Al_3Li$ precipitates in binary Al-Li alloys using TEM to obtain microscopic details. Abis *et al.* [32] studied phase coarsening in Al-Li alloys using small-angle neutron scattering experiments. Che and Hoyt [33] extended the phase coarsening model of Marder [16] and derived a form for the scaled structure function based on it. Che *et al.* [34] studied phase coarsening in Al-Li alloys using small-angle x-ray scattering experiments.

In summary, by contrast, the three-dimensional microstructure images and movies provided here can be used for a more direct comparison with that from future physical experiments. Spatial correlations within the microstructure were carefully studied, and the results reported here show that the interparticle spacings in two-phase dispersed systems predicted from the analytic approximation of Bansal and Ardell are the most accurate. Therefore, these findings conclude a long-standing controversy in the calculation of interparticle spacing. Voronoi cells constructed for the case of $V_V=0.1$ capture details of the locale, and relate to the particle's growth rate and volume flux. A three-dimensional Voronoi network movie shows the dynamic processes affecting the local environment of every particle. Moreover, the present simulations permit determination of the growth rates of individual particles, and show that there exist locale fluctuations in the growth rate of individual particles during microstructure evolution, for both sparse finite microstructures as well as for moderately dense ones. Simulations and Eq. (10) indicate that larger particles experience stronger fluctuations than do smaller ones, and systems with higher volume fractions experience stronger fluctuations than do sparse systems. Locale fluctuations can be described approximately by multiplicative Gaussian noise—a finding, now well supported by high-accuracy multiparticle simulations.

The authors are pleased to acknowledge partial financial support received from the NASA, Marshall Space Flight Center, under Grant No. NAG-8-1468.

[1] X. Peng *et al.*, Nature (London) **404**, 59 (2000).
[2] V. F. Puntes, K. M. Krishnan, and A. P. Alivisatos, Science **291**, 2115 (2001).
[3] B. Liu and H. C. Zeng, Small **1**, 566 (2005).
[4] T. Müller, K. H. Heinig, and W. Möller, Appl. Phys. Lett. **81**, 309 (2002).
[5] P. P. Bansal and A. J. Ardell, Metallography **5**, 97 (1972).
[6] J. W. Martin, *Precipitation Hardening*, 2nd ed. (Butterworth-Heinemann, Oxford, 1998), pp. 58–59, 81.
[7] A. V. Nadkarni, in *High Conductivity Coper and Aluminum Alloys*, edited by E. Ling and P. W. Taubenblat (Metall. Soc. AIME, Warrendale, PA, 1984), pp. 77–101.
[8] G. E. Dieter, *Mechanical Metallurgy*, 3rd ed. (McGraw-Hill, New York, 1986), p. 215.
[9] I. M. Lifshitz and V. V. Slyozov, J. Phys. Chem. Solids **19**, 35 (1961).
[10] C. Wagner, Z. Elektrochem. **65**, 581 (1961).
[11] A. J. Ardell, Acta Metall. **20**, 61 (1972).
[12] K. Tsumuraya and Y. Miyata, Acta Metall. **31**, 437 (1983).
[13] A. D. Brailsford and P. Wynblatt, Acta Metall. **27**, 489 (1979).
[14] S. P. Marsh and M. E. Glicksman, Acta Mater. **44**, 3761 (1996).
[15] J. A. Marqusee and J. Ross, J. Chem. Phys. **80**, 536 (1984).
[16] M. Marder, Phys. Rev. A **36**, 858 (1987).
[17] K. Kawasaki and T. Ohta, Physica A **118A**, 175 (1983).
[18] M. Tokuyama and Kawasaki, Physica A **123A**, 386 (1984).
[19] K. Kawasaki, Y. Enomoto, and M. Tokuyama, Physica A **135A**, 426 (1986).
[20] Y. Enomoto, M. Tokuyama, and K. Kawasaki, Acta Metall. **34**, 2119 (1986).
[21] K. G. Wang, M. E. Glicksman, and K. Rajan, Phys. Rev. E **69**, 061507 (2004).
[22] J. Weins and J. W. Cahn, in *Sintering and Related Phenomena*, edited by G. C. Kuczynski (Plenum, New York, 1973), pp. 151–163.
[23] P. W. Voorhees and M. E. Glicksman, Acta Metall. **32**, 2013 (1984).
[24] C. W. J. Beenakker, Phys. Rev. A **33**, 4482 (1986).
[25] N. Akaiwa and P. W. Voorhees, Phys. Rev. E **49**, 3860 (1994).
[26] M. Tokuyama and Y. Enomoto, Phys. Rev. E **47**, 1156 (1993).
[27] K. G. Wang and M. E. Glicksman, Phys. Rev. E **68**, 051501 (2003).
[28] N. C. Bartelt *et al.*, Phys. Rev. B **54**, 11741 (1996).
[29] J. R. Rogers *et al.*, J. Electron. Mater. **23**, 999 (1994).
[30] B. P. Gu, G. L. Liedl, J. H. Kulwicki, and T. H. Sanders, Jr., Mater. Sci. Eng. **70**, 217 (1985).
[31] K. Mahalingam *et al.*, Acta Metall. **35**, 483 (1987).
[32] S. Abis *et al.*, Phys. Rev. B **42**, 2275 (1990).
[33] D. Z. Che and J. J. Hoyt, Acta Metall. Mater. **43**, 2551 (1995).
[34] D. Z. Che, S. Spooner, and J. J. Hoyt, Acta Mater. **45**, 1167 (1997).